Thermo-economic analysis and multi-objective optimization of vapour cascade refrigeration system using different refrigerant combination

A comparative study

Ranendra Roy[1] · Bijan Kumar Mandal[1]

Abstract

A numerical investigation of energetic, exergetic, economic and environmental performances of a 50-kW cooling capacity cascade refrigeration system using four different refrigerant pairs, namely R41–R404A, R170–R404A, R41–R161 and R170–R161, has been carried out. Effects of evaporator temperature, condenser temperature, LTC condenser temperature and cascade condenser temperature difference have been studied parametrically. The COP and exergetic efficiency of the system are found to be maximum with R41–R161 refrigerant pair followed by R170–R161 for the same operating conditions. Genetic algorithm technique has been employed to carry out multi-objective optimization for the cascade refrigeration system using above-mentioned four refrigerant pairs to evaluate the optimal performances (for maximizing exergetic efficiency and minimizing the total plant cost rate) and the corresponding operating conditions. A set of non-dominated solutions have been obtained from the optimization, and then, TOPSIS method is employed to get the unique solutions for all four investigated refrigerant pairs. Better results in terms of optimum exergetic efficiency and the total plant cost rate are obtained using R41–R161 and R170–R161 refrigerant pairs compared to those obtained using R41–R404A pair.

Keywords Cascade refrigeration · Exergetic efficiency · Cost · Multi-objective optimization · TOPSIS

List of symbols

A	Area
C	Capital cost
$\dot{C}$	Cost rate
COP	Coefficient of performance
CRF	Capital recovery factor
E	Annual energy consumption
ED	Exergy destruction
Ex	Exergy
h	Enthalpy
HTC	High-temperature circuit
i	Interest rate
LMTD	Logarithmic mean temperature difference
LTC	Low-temperature circuit
$\dot{m}$	Mass flow rate
n	Plant life
N	Annual operational hour
s	Entropy
T	Temperature
U	Overall heat transfer coefficient
W	Work input

Greek symbols

α	Cost
η	Efficiency
μ	Emission factor
φ	Maintenance factor

Subscripts

cas	Cascade condenser
comp,h	HTC compressor
comp,l	LTC compressor

✉ Ranendra Roy
  ranendraroy2009@gmail.com

  Bijan Kumar Mandal
  bkm375@yahoo.co.in

[1] Department of Mechanical Engineering, Indian Institute of Engineering Science and Technology, Shibpur, Howrah, West Bengal 711103, India

cond	Condenser
elec	Electrical
eva	Evaporator
exp,h	HTC expansion valve
exp,l	LTC expansion valve
m	Mechanical
s	Isentropic

Introduction

The increasing energy demand for refrigeration and air conditioning in developing countries and the environmental impact of some commonly used refrigerants motivated many researchers to develop energy-efficient refrigeration systems using environment-friendly refrigerants. The recent report of IIR shows that about 17% of the total world energy consumption is being utilized in refrigeration sectors [1]. There are many applications of refrigeration in ice industries, chemical industries and frozen food industries, where the temperature lift can be quite high either due to the requirement of very low evaporator temperatures or due to very high condensing temperatures at hotter climatic regions. Under such situations, the use of simple single-stage vapour compression refrigeration system is not desirable as it leads to a decrease in cooling effect, an increase in compressor power and wear and tear of the compressor. One of the methods to overcome the high-temperature lift problem is the use of cascade refrigeration system (CRS) [2]. Also, the report of the recent Kigali amendment in 2016 [3] initiated the phase out of refrigerants having high global warming potential (GWP). This motivated researchers to look for new alternative refrigerants as replacement of refrigerants having relatively high GWP.

Kilicarslan [4] investigated a two-stage vapour compression CRS using different amounts of R134 as the refrigerant in both the LTC and HTC and achieved higher COP compared to the single-stage system. Nicola et al. [5] presented a thermodynamic analysis of CRS operating with the blends of R744 and various HFC refrigerants in the low-temperature circuit and R717 in the high-temperature circuit. They found the blends of HFC with R744 as suitable alternative refrigerants for very low temperature applications. Niu and Zhang [6] reported that the blend of R744 and R290 was capable of replacing R13 in the LTC. Few researchers [7–10] investigated on CO_2–NH_3 CRS to evaluate the optimal operating conditions in order to achieve the maximum thermodynamic performance of the system. An energy analysis on a R744–R717 CRS was performed by Messineo [11] and compared with a HFC refrigerant R404A-based two-stage refrigeration system. R744–R717 CRS was noted to perform better than a R404A-based two-stage refrigeration system for low-temperature applications so far as the

energy, security and environmental aspects were concerned. Kilicarslan and Hosez [12] observed a decrease in COP and an increase in irreversibility with the rise in cascade condenser temperature difference. Experimental works [13–16] showed the use of R744–R717 refrigerant pair to be effective for low-temperature applications. Few more experimental studies [17–19] are also available on R744–R717 CRS for supermarket applications. Ouadha et al. [20] conducted a numerical study and recommended R744–R717 as one of the best refrigerant pairs to be used in CRS for low-temperature applications. Cabello et al. [21] experimented on a cascade refrigeration system using refrigerant R152a and R134a in the LTC and R744 in the HTC. They reported that the use of R152a in LTC instead of R134a yielded better performances. Sun et al. [22] simulated a CRS using R41–R404A and R23–R404A as refrigerant combinations and found the system to give better performance using R41–R404A refrigerant pair. Roy and Mandal [23, 24] proposed R170 and R161 instead of R41 and R404A, respectively, for CRS considering thermodynamic aspects. Rezayan and Behbahaninia [25] studied the influence of evaporator, condenser, LTC condenser temperature and the temperature difference in cascade condenser on the total plant cost rate of a R744–R717 based CRS. Mosaffa et al. [26] performed exergoeconomic and environmental analyses on CRS with two different configurations and compared. Aminyavari et al. [27] performed multi-objective optimization on a R744–R717 CRS. To combat the ozone depletion in the stratosphere due to the leakage and dispersion of CFC- and HCFC-based refrigerants, R134a was introduced as the short-term substitute of chlorine-based halogenated refrigerants. Afterwards, it was observed that R134a has relatively high GWP and researchers tried to find alternative to this. Abraham and Mohanraj [28] experimented on an automobile air conditioner using R430A as a substitute of R134a and obtained better thermodynamic performance also. Gill et al. [29] in their experimental study on a vapour compression refrigeration system noted improvement in the performance using R134a/LPG blend instead of R134a. They also developed artificial neural network (ANN) model to predict the second law efficiency and total irreversibility of the system. In other experimental works, Gill et al. [30, 31] experimentally investigated on vapour compression refrigeration system using R450A and LPG/TiO_2–lubricant and suggested refrigerant R450A as the substitute of R134a. Paradeshi et al. [32, 33] studied the performance of a direct-expansion solar-assisted heat pump and concluded that refrigerants R290 and R433A might be used as possible energy-efficient alternatives to R22. Esfe et al. [34] carried out optimization of nanofluid flow in double-tube heat exchangers employing genetic algorithm considering the heat transfer coefficient and the cost as the two objective functions. Esfe et al. [35–37] estimated thermal conductivity of Al_2O_3 nanoparticles in

water–ethylene glycol solution using experimental data and established a correlation using feedforward multi-layer perceptron (MLP) artificial neural network (ANN). In another study, Shahsavar et al. [38] conducted experimental investigation to study the effect of temperature, nanoparticle mass concentration and surfactant concentration on the thermal conductivity and the viscosity of liquid paraffin–Al_2O_3 nanofluid containing oleic acid surfactant. Few more studies [39–41] had also been carried out employing ANN to predict the thermal conductivity of MgO–ethylene glycol and Fe_3O_4 nanofluids and dynamic viscosity of TiO_2 nanofluids. Ahmadi and Toghraie [42, 43] carried out thermodynamic analysis of Shahid Montazeri power plant and estimated energy and exergy efficiencies for three different cases. Ahmadi et al. [44–47] also presented different case studies on different power plants in Iran considering energetic, exergetic, economic and environmental aspects. Under current scenario, all refrigeration system should also be analysed giving importance to the economic and environmental issues in addition to thermodynamic aspects.

Though substantial amount of experimental and numerical works are available in the literature on CRS, there is a gap considering today's requirements. To protect the environment from further degradation, the refrigerants used in any system must have zero ODP and very low GWP. Most of the published research papers have dealt with CO_2–NH_3 as refrigerant pair having zero ODP and low GWP. It will be interesting to investigate CRS using refrigerant pairs of hydrocarbon and HFC having low GWP. On the other hand, several previous studies on CRS have mainly focused on the thermodynamic performance of the system. Very limited amount of works have been found addressing the economic performance of the system. It is also observed that the influence of different design parameters on the thermodynamic as well as economic performances, i.e. COP, exergetic efficiency and total plant cost rate of the system, has not been addressed properly. Works related to the application of multi-criteria decision-making (MCDM) in CRS are also very limited.

The present work is mainly focused on the impact of different design parameters on the COP, exergetic efficiency and total cost rate of the system using four refrigerant combinations. An attempt has been made to replace refrigerant combination R41–R404A proposed by Sun et al. [22] with some other refrigerant combinations having lower GWP and better thermo-economic performances. Multi-objective optimization considering exergetic efficiency and total plant cost as two objective functions has also been carried out to find out the non-dominated solutions, and then, a decision-making technique, TOPSIS, is employed to determine the unique solution from the optimization results.

System description

The schematic diagram of a typical CRS and the corresponding p–h plot are shown in Fig. 1a, b, respectively. In CRS, two single-stage vapour compression refrigeration cycles are connected with each other in series through a cascade heat exchanger. This cascade heat exchanger serves as condenser for the low-temperature circuit (LTC) and as evaporator for the high-temperature circuit (HTC). In the cascade heat exchanger, the LTC refrigerant rejects the heat which is absorbed by HTC refrigerant. Refrigerants R41 and R170 are selected for the LTC and R404A and R161 are chosen for HTC separately. The thermophysical properties of different refrigerants considered in this work are listed in Table 1 [48].

In the evaporator, Q_{eva} amount of heat is absorbed by the LTC refrigerant at evaporator temperature of T_{eva} and gets evaporated. The vapour refrigerant then enters the LTC compressor (state 1), where W_{LTC} amount of work is supplied to raise its temperature and pressure (state 2). It is then sent to the cascade heat exchanger where LTC refrigerant rejects Q_{cas} amount of heat at LTC condenser temperature, T_{LC} which is absorbed by the HTC refrigerant at HTC evaporator temperature, T_{HE}. This causes condensation (state 3) of the LTC refrigerant and evaporation (state 5) of the HTC refrigerant. The condensed LTC refrigerant then enters the LTC throttle device and expanded to the evaporator pressure (state 4) and enters the evaporator. The vapourized HTC refrigerant, coming out from the cascade heat exchanger, enters the HTC compressor. W_{HTC} amount of work is consumed by the HTC compressor to compress the refrigerant to the condenser pressure, and this compressed and superheated refrigerant enters the condenser at state 6. The refrigerant vapour is first desuperheated and then condensed to saturated liquid (state 7) at condenser temperature of T_{cond} by rejecting Q_{cond} amount of heat. The condensed HTC refrigerant is then passed through the HTC throttle device and expands to the HTC evaporator pressure at state 8. The evaporator temperature, condenser temperature, LTC condenser temperature and the temperature difference in the cascade heat exchanger are the four most important parameters which have great influence on the performance of system.

Mathematical modelling

A mathematical model has been developed based on the equations available in the literature for the analysis of CRS from thermodynamic and economic point of view. However, following assumptions have been made to make the overall analysis simplified and feasible:
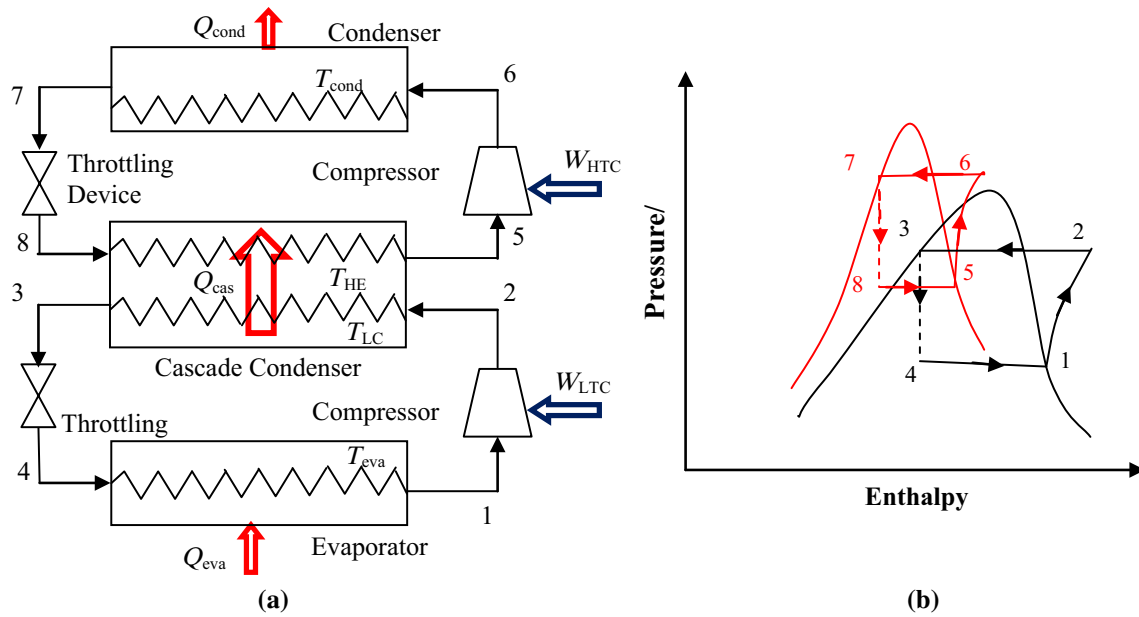
Fig. 1 Representation of CRS **a** schematic diagram and **b** *P–h* diagram

Table 1 Thermo-physical properties of R170, R41, R161 and R404A [48]

Refrigerant	Molecular mass/g mol^{-1}	Critical temperature/°C	Boiling point/°C	ASHRAE safety code	ODP	GWP
R170	30.07	32.2	− 88.9	A3	0	∼ 20
R41	34.03	44.1	− 78.1	A2	0	97
R161	48.06	102.2	− 37.1	A3	0	12
R404A	97.6	72.1	− 46.6	A1	0	3800

- Pressure drops and heat losses in the components and in the pipe lines are neglected.
- Kinetic and potential energies are not considered.
- No subcooling is considered for both the cycles.
- Isentropic efficiencies of the compressors are independent of pressure ratio in both the cycles.
- All the components are operating at a steady-state condition.

Energy and exergy analysis

Based on the above-said assumptions, mass, energy and exergy balance equations are applied to all the components to estimate the overall performance of the system. Those equations for all the components of the system are summarized in Table 2.

Now, the total compressor power requirement can be calculated as:

$$W_{\text{Total}} = W_{\text{LTC}} + W_{\text{HTC}} \tag{1}$$

Overall COP of the system is given by

$$\text{COP} = \frac{Q_{\text{eva}}}{W_{\text{Total}}} \tag{2}$$

Heat transfer area of evaporator, condenser and cascade condenser can be calculated following Mosaffa et al. [26] and Navidbakhsh et al. [51] as:

$$A = \frac{Q}{U \times \text{LMTD}} \tag{3}$$

Exergy is defined as the maximum obtainable work from any system. Exergy at any point of the system can be obtained as:

$$\text{Ex} = \dot{m}[(h - h_0) - T_0(s - s_0)] \tag{4}$$

Total exergy destruction is the sum of exergy destructions in various components of the system and can be written as:

$$\begin{aligned} \text{ED}_{\text{Total}} = {} & \text{ED}_{\text{eva}} + \text{ED}_{\text{comp,l}} + \text{ED}_{\text{exp,l}} + \text{ED}_{\text{comp,h}} \\ & + \text{ED}_{\text{exp,h}} + \text{ED}_{\text{cas}} + \text{ED}_{\text{cond}} \end{aligned} \tag{5}$$

Exergetic efficiency of the system can be expressed following Dincer et al. [52] as:

Table 2 Mass, energy and exergy balance equations of individual components of CRS [49, 50]

Components	Mass balance	Energy balance	Exergy balance
Evaporator	$\dot{m}_4 = \dot{m}_1 = \dot{m}_{LTC}$ $\dot{m}_{LTC} = \dfrac{Q_{eva}}{h_1 - h_4}$	$Q_{eva} = \dot{m}_{LTC}(h_1 - h_4)$	$ED_{eva} = Ex_4 - Ex_1 + Q_{eva} \times \left(1 - \dfrac{T_0}{T_{eva}}\right)$
LTC compressor	$\dot{m}_1 = \dot{m}_2 = \dot{m}_{LTC}$	$W_{LTC} = \dfrac{\dot{m}_{LTC}(h_2 - h_1)}{\eta_S \times \eta_m \times \eta_{elec}}$	$ED_{comp,l} = Ex_1 - Ex_2 + W_{LTC}$
Cascade condenser	$\dot{m}_2 = \dot{m}_3 = \dot{m}_{LTC}$ $\dot{m}_8 = \dot{m}_5 = \dot{m}_{HTC}$	$Q_{cas} = \dot{m}_{LTC}(h_2 - h_3)$ $= \dot{m}_{HTC}(h_5 - h_8)$	$ED_{cas} = Ex_2 + Ex_8 - Ex_3 - Ex_5$
LTC throttle valve	$\dot{m}_3 = \dot{m}_4 = \dot{m}_{LTC}$	$h_3 = h_4$	$ED_{exp,l} = Ex_3 - Ex_4$
HTC compressor	$\dot{m}_5 = \dot{m}_6 = \dot{m}_{HTC}$	$W_{HTC} = \dfrac{\dot{m}_{HTC}(h_6 - h_5)}{\eta_S \times \eta_m \times \eta_{elec}}$	$ED_{comp,h} = Ex_5 - Ex_6 + W_{HTC}$
HTC throttle valve	$\dot{m}_7 = \dot{m}_8 = \dot{m}_{HTC}$	$h_7 = h_8$	$ED_{exp,h} = Ex_7 - Ex_8$
Condenser	$\dot{m}_6 = \dot{m}_7 = \dot{m}_{HTC}$	$Q_{cond} = \dot{m}_{HTC}(h_6 - h_7)$	$ED_{cond} = Ex_6 - Ex_7 - Q_{cond} \times \left(1 - \dfrac{T_0}{T_{cond}}\right)$

$$\eta_{ex} = \frac{W_{Total} - ED_{Total}}{W_{Total}} \tag{6}$$

Economic analysis

The first step in the economic analysis is to identify the different costs involved in the system. Total plant cost rate involves the costs associated with capital and maintenance cost rate ($\sum_k \dot{C}_k$), operational cost rate ($\dot{C}_{OP}$) and the penalty cost rate due to CO_2 emission ($\dot{C}_{env}$). Total cost rate is the sum of total capital and maintenance cost rate, operational cost rate and the penalty cost due to CO_2 emission of the system. So, total plant cost rate of the CRS can be written as:

$$\dot{C}_{Total} = \sum_k \dot{C}_k + \dot{C}_{OP} + \dot{C}_{env} \tag{7}$$

The capital costs of different components in the system are estimated based on the cost functions as listed in Table 3. The cost functions for different components of the system are taken from the work of Mosaffa et al. [26] and Aminyavari et al. [27].

The rate of capital investment and maintenance cost of each component of the system can be estimated as:

$$\dot{C}_k = C_k \times \varphi \times CRF \tag{8}$$

Again, CRF is calculated from the following equation [52, 53]

$$CRF = \frac{i(i+1)^n}{(1+i)^n - 1} \tag{9}$$

Total capital investment and maintenance cost rate of the whole system can be calculated by adding the capital investment and maintenance costs of all components, and it is given by

Table 3 Cost functions of the system components [26, 27]

Component	Capital cost function
HTC compressor	$C_{comp,h} = 9624.2 \times W_{HTC}^{0.46}$
LTC compressor	$C_{comp,l} = 10,167.5 \times W_{LTC}^{0.46}$
HTC throttle valve	$C_{exp,h} = 114.5 \times \dot{m}_{HTC}$
LTC throttle valve	$C_{exp,l} = 114.5 \times \dot{m}_{LTC}$
Evaporator	$C_{eva} = 1397 \times A_{eva}^{0.89}$
Condenser	$C_{cond} = 1397 \times A_{cond}^{0.89}$
Cascade condenser	$C_{cas} = 383.5 \times A_{cas}^{0.65}$

$$\sum_k \dot{C}_k = \dot{C}_{eva} + \dot{C}_{cond} + \dot{C}_{cas} + \dot{C}_{comp,l} + \dot{C}_{comp,h} + \dot{C}_{exp,h} + \dot{C}_{exp,l} \tag{10}$$

Operational cost of the system includes the cost of electricity consumption by the compressor and can be expressed as:

$$\dot{C}_{OP} = N \times W_{Total} \times \alpha_{elec} \tag{11}$$

Environmental analysis

The rate of penalty cost due to GHG emission for the CRS can be estimated following Wang et al. [54] as:

$$\dot{C}_{env} = m_{CO_2e} \times C_{CO_2} \tag{12}$$

Amount of annual GHG emission from the system (m_{CO_2e}) can be calculated as [54]:

$$m_{CO_2e} = \mu_{CO_2e} \times E_{annual} \tag{13}$$

Values of some input parameters have been assumed for the complete analysis of the system, and those are listed in Table 4.

Validation of the numerical work

A mathematical model has been developed in engineering equation solver [55] for the simulation of cascade refrigeration system using the equations as mentioned in the earlier section. The validity of the basic mathematical model used for this simulation work has been established by comparing the predicted results with the experimental results of Sawalha et al. [56] for a CO_2/NH_3 cascade system refrigeration system. The model has been validated with the experimental data for evaporator temperature of $-26\,°C$, LTC condenser temperature of $-9\,°C$, HTC evaporator temperature of $-11\,°C$ and condenser temperature of $32\,°C$. The different efficiencies of the LTC and HTC compressors are taken as: $\eta_{S,LTC} = 21\%$, $\eta_{m,LTC} = 93\%$, $\eta_{elec,LTC} = 80\%$, $\eta_{S,HTC} = 76\%$, $\eta_{m,HTC} = 93\%$ and $\eta_{elec,HTC} = 80\%$. No subcooling is considered for any stage, and 7 K of superheating in LTC has been considered. The work input to the LTC compressor and COPs in both LTC and HTC from the present study is compared with the experimental results of Sawalha et al. [56]. The predicted results match well quantitatively with the experimental results for all three parameters. The percentage deviations between experimental results and numerical values are also calculated, and those are found to

be 2.1%, 1.7% and 9% for work input to the LTC compressor and COPs in both LTC and HTC, respectively. The analysis of different important performance parameters has been carried out by running the code in EES at different operating conditions for the investigated refrigerant combinations.

System optimization

Multi-objective optimization

Multi-objective optimization is a method for solving optimization problems having conflicting objectives such as minimizing cost and maximizing performance simultaneously. Generally, multi-objective optimization does not result in a unique solution which can satisfy all the objective functions. A multi-objective optimization results in a set of optimal solutions where all of them can satisfy all the objectives at reasonable level. Those set of solutions are named as Pareto optimal solutions. After obtaining these Pareto solutions, decision maker decides the best solution among all the solutions using different decision-making techniques. In this study, a multi-objective optimization has been carried out using multi-objective genetic

Table 4 Basic assumptions for the simulation

Parameters	Values
Cooling load, Q_{eva}	50 kW
Both compressors isentropic efficiency, η_S	80%
Both compressors mechanical efficiency, η_m	100%
Both compressors electrical efficiency, η_{elec}	100%
Dead state temperature, T_0	25 °C
Condenser temperature, T_{cond}	37–55 °C
Evaporator temperature, T_{eva}	$-50\,°C$ to $-21\,°C$
Temperature difference in cascade condenser, ΔT	2–8 °C
LTC condenser temperature, T_{LC}	$-6\,°C$ to 6 °C
Superheating in LTC	5 °C
Superheating in HTC	5 °C
Overall heat transfer coefficient of evaporator	$0.03\ kW\ m^{-2}\ K^{-1}$
Overall heat transfer coefficient of condenser	$0.04\ kW\ m^{-2}\ K^{-1}$
Overall heat transfer coefficient of cascade condenser	$1\ kW\ m^{-2}\ K^{-1}$
Temperature difference of air in evaporator and condenser	10 K
Temperature of the inlet air to the evaporator	$-10\,°C$
Maintenance factor, ϕ	1.06
Interest rate, i	14%
Plant life time, n	15 years
Annual operational hour, N	4266 h
Electrical power cost, α_{el}	0.09 USD/kW h
Emission factor, μ_{CO_2e}	0.968 kg/kW h
Cost of CO_2 avoided, C_{CO_2}	0.09 USD/kg of CO_2 emission

algorithm (MOGA) [57, 58] in MATLAB optimization toolbox. After this, technique for order of preference by similarity to ideal solution (TOPSIS) [59, 60] is implemented to find the best solution (among the Pareto optimal set) that satisfies the requirement of the current problem. A multi-objective optimization problem can be expressed mathematically as follows:

$$\text{Find } x = (x_i) \quad \forall i = 1, 2, 3 \ldots N_{\text{par}} \tag{13}$$

$$\text{Minimize or maximize } f_i(x), \quad \forall i = 1, 2, 3, \ldots N_{\text{obj}} \tag{14}$$

$$g_j(x) = 0, \quad \forall j = 1, 2, 3, \ldots, m \tag{15}$$

$$h_k(x) = 0, \ldots \forall k = 1, 2, 3, \ldots, n \tag{16}$$

where x, N_{par}, $f_i(x)$, N_{obj}, $g_j(x)$ and $h_k(x)$ are the decision variables vectors, number of decision variables, objectives, number of objectives, equality and inequality constraints, respectively. For the present work, two parameters, exergetic efficiency and total plant cost rate, are chosen as objective functions for multi-objective optimization. The aim of the optimization is to maximize exergetic efficiency and minimize the total plant cost rate. Model building for both objective functions has been carried out using Box–Behnken method in Minitab software [61]. The decision variable vectors and their ranges are given in Table 5.

TOPSIS decision-making

Technique for order preference by similarity to ideal solution (TOPSIS) is a very popular and unique method for multi-criteria decision-making. This method is applied to get the unique optimal solution. The steps for TOPSIS decision-making are as follows [60]:

STEP 1 Creation of an evaluation matrix with m alternatives and n criteria.

$$\begin{bmatrix} a_{11} \cdots a_{1j} \cdots a_{1n} \\ \vdots \quad \vdots \quad \vdots \\ a_{i1} \cdots a_{ij} \cdots a_{in} \\ \vdots \quad \vdots \quad \vdots \\ a_{m1} \cdots a_{mj} \cdots a_{mn} \end{bmatrix}$$

STEP 2 Normalization of the evaluation matrix using the following equation:

$$a_{ij} = \frac{a_{ij}}{\sqrt{\sum\limits_{i=1}^{m} a_{ij}^2}} \tag{17}$$

Table 5 Design parameters for optimization and their ranges

Design parameters	Range
Evaporator temperature/°C	$-50 \leq T_{\text{eva}} \leq -21$
Condenser temperature/°C	$37 \leq T_{\text{cond}} \leq 55$
LTC condenser temperature/°C	$-6 \leq T_{\text{LC}} \leq 6$
Cascade condenser temperature difference/K	$2 \leq \Delta T \leq 8$

STEP 3 Determination of the weighted matrix by multiplying the mass factor with the normalized matrix as follows:

$$V_{ij} = w_i \times a_{ij} \tag{18}$$

STEP 4 Determination of positive and negative ideal solutions.

$$A_j^+ = \left\{ \text{Max } V_{ij} | j \in K \right\}, \left\{ \text{Min } V_{ij} | j \in K' \right\} \tag{19}$$

$$A_j^- = \left\{ \text{Min } V_{ij} | j \in K \right\}, \left\{ \text{Max } V_{ij} | j \in K' \right\} \tag{20}$$

where K is the benefit parameters and K' is the non-benefit parameters or cost parameters.

STEP 5 Calculation of distances from positive and negative ideal solutions from the given equations.

$$S_i^+ = \sqrt{\sum_{j=1}^{n} (V_{ij} - A_j^+)^2} \tag{21}$$

$$S_i^- = \sqrt{\sum_{j=1}^{n} (V_{ij} - A_j^-)^2} \tag{22}$$

STEP 6 Determination of relative closeness from the ideal solution can be expressed as:

$$C_i = \frac{S_j^-}{S_j^+ + S_j^-} \tag{23}$$

Rank C_i in descending order where highest value gives the ideal solution.

The results from the multi-objective optimization, i.e. the Pareto optimal set of solutions, undergo these aforementioned steps, and the ranks are assigned. Finally, a unique solution among the Pareto solutions is chosen based on the rank obtained from the TOPSIS method.

Results and discussion

The CRS has been investigated numerically using four refrigerant pairs, namely R41–R404A, R170–R404A, R41–R161 and R170–R161, on energy, exergy and economy basis. The influence of several parameters such as evaporator temperature, condenser temperature, LTC condenser temperature and temperature difference in the cascade condenser on the performance of the system has been analysed. Finally, multi-objective optimization technique using genetic algorithm and TOPSIS method are employed to obtain the optimal point for the system using each refrigerant pair.

Effect of evaporator temperature on COP and exergetic efficiency

Figure 2 shows the effect of evaporator temperature on COP and exergetic efficiency of the system for the investigated refrigerant pairs keeping condenser temperature, LTC condenser temperature and the temperature difference in cascade condenser constant at 40 °C, 6 °C and 5 K, respectively. It shows that both COP and exergetic efficiency of the system increase with the increase in evaporator temperature for all the refrigerant pairs. As the evaporator temperature increases, the temperature lift and hence the pressure ratio in the LTC decreases. As a result, the compressor power and also the total exergy destruction decrease. The reductions in both compressor power and exergy destruction finally lead to the increase in the overall COP and exergetic efficiency of the system. Both the COP and the exergetic efficiency achieved with the system using
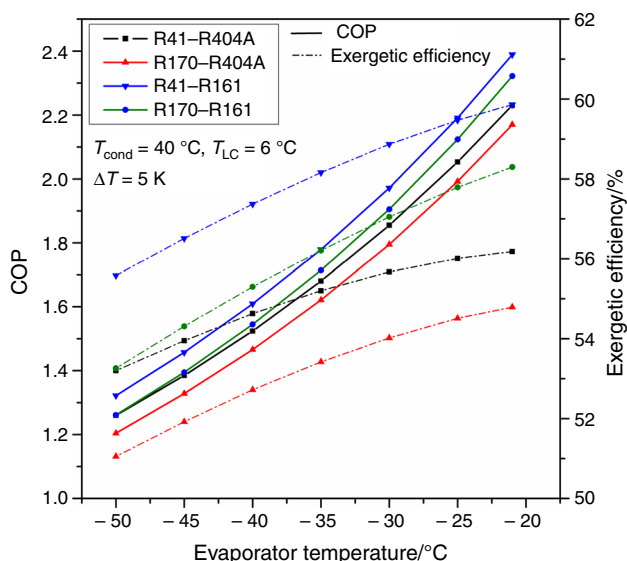
R41–R161 refrigerant pair are found to be the best due to better thermodynamics performance of refrigerant R161 [62–65]. Thermodynamic performances obtained with R170–R404A pair for the entire evaporator temperature range considered in this work are lower compared to those using other refrigerant pairs. It can be noted from the figure that the COP obtained at evaporator temperature of −21 °C using R41–R404A, R170–R404A, R41–R161 and R170–R161 as refrigerant pairs is 2.23, 2.17, 2.39 and 2.32, respectively. The differences in exergetic efficiency of the system between R170–R161 and R41–R161 have been calculated within the investigated evaporator temperature range. The values are found to be 2.7% and 4.4% at evaporator temperatures of − 21 °C and − 50 °C, respectively, for the fixed values of other temperatures as mentioned above.

Effect of evaporator temperature on total plant cost

The variations of total plant cost rate with evaporator temperature are presented in Fig. 3 for the four refrigerant pairs keeping condenser temperature, LTC condenser temperature and the temperature difference in cascade condenser constant at 40 °C, 6 °C and 5 K, respectively. It can be observed from the figure that the total plant cost initially decreases and after a certain point it starts to increase with the increase in evaporator temperature. This is due to the fact that as the evaporator temperature increases compressor power requirement decreases which causes a decrement in the operational cost and the CO_2

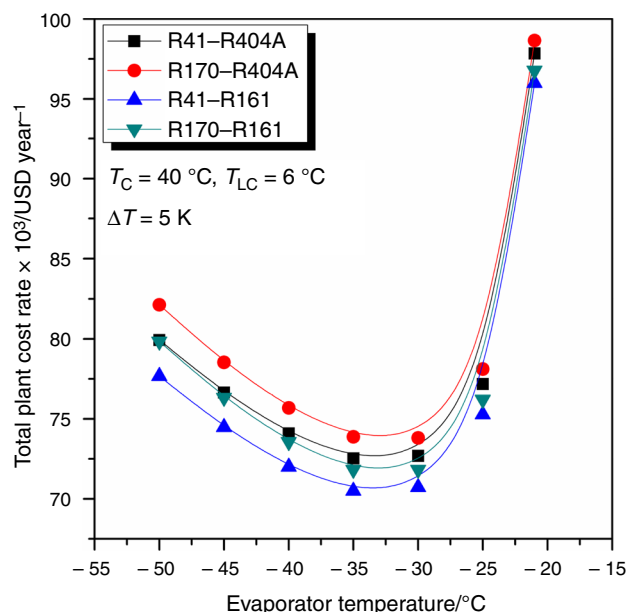Fig. 2 Effect of evaporator temperature on COP and exergetic efficiency of the system

Fig. 3 Effect of evaporator temperature on total plant cost rate of the system

penalty cost. But, at the same time, this increases the capital and maintenance cost due to the increase in evaporator heat transfer area. Capital and maintenance cost increases rapidly beyond a certain evaporator temperature (around -30 °C) and results in an increase in the total plant cost rate. Plant cost is least when the system is operated with R41–R161 refrigerant pair and plant cost becomes maximum when the system works using R170–R404A refrigerant pair. Plant cost rate for the system using R170–R161 is slightly higher than the system using R41–R161 refrigerant pair. However, required plant cost rate using refrigerant pairs R41–R161 and R170–R161 is slightly lower than that using refrigerant pair R41–R404A. Difference in total plant cost between the system working with R41–R161 and R170–R161 pair has been evaluated, and it is noted to change only by 0.8–2.7% when the evaporator temperature is decreased from -21 to -50 °C.

Effect of condenser temperature on COP and exergetic efficiency

The variations of the COP and the exergetic efficiency of the system with condenser temperature are shown in Fig. 4. The simulations have been carried out keeping the other operating parameters, i.e. evaporator temperature, LTC condenser temperature and cascade condenser temperature difference fixed at -35 °C, 6 °C and 5 K, respectively. Figure shows that both the COP and the exergetic efficiency decrease with the increase in condenser temperature due to the increase in pressure ratio in HTC and the total compressor power. The figure also shows that the
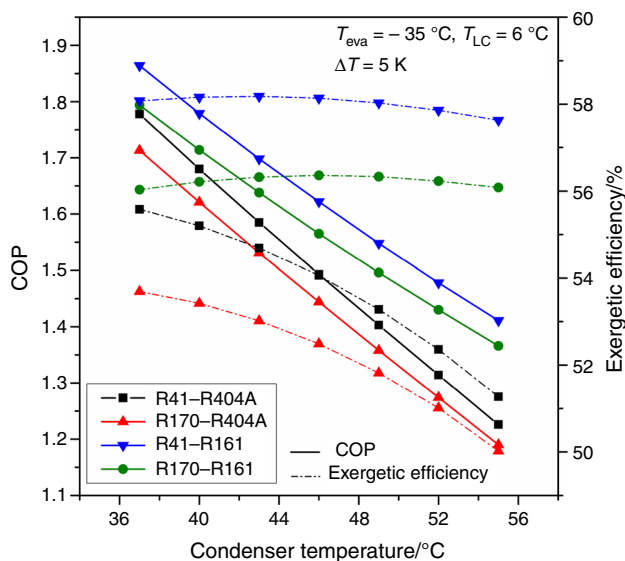
maximum COP and the exergetic efficiency are obtained using the refrigerant pair R41–R161 and these are minimum using refrigerant pair R170–R404A. It may be noted that refrigerant pair R170–R161 is comparable to R41–R161 combination in terms of COP and exergetic efficiency. However, the performance deteriorates slightly with R170–R161 pair. It may also be noted that performances obtained using refrigerant pairs R41–R161 and R170–R161 are slightly higher compared to those using refrigerant pair R41–R404A. Predicted results show 3.9–3.3% higher COP and 3.7–2.8% higher exergetic efficiency with the system using R41–R161 pair compared to the system using R170–R161 pair when the condenser temperature is increased from 37 to 55 °C.

Effect of condenser temperature on total plant cost

Figure 5 presents the effect of condenser temperature on total plant cost rate for all four refrigerant pairs. The total plant cost initially decreases up to a certain condenser temperature (in the range of 46–50 °C) of condenser, but beyond that the plant cost rate starts to increase. As the condenser temperature increases, compressor power increases. This leads to an increase in the plant operational cost as well as CO_2 penalty cost. But, an increase in condenser temperature causes a reduction in overall heat transfer area for the condenser which results in a decrease in the condenser cost and hence the total capital and maintenance cost of the plant. The combined sum of operational cost and CO_2 penalty cost becomes higher than the total capital and maintenance cost of the plant beyond a certain condenser temperature. This leads to an increase in the total plant cost of the system. It has been observed that
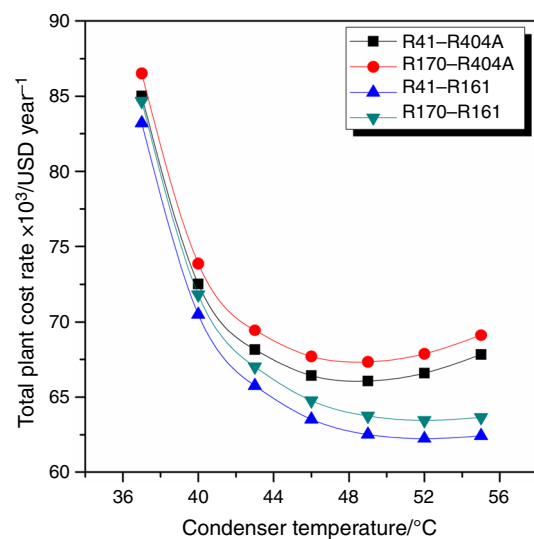

Fig. 4 Effect of condenser temperature on COP and exergetic efficiency of the system

Fig. 5 Variation of total plant cost rate on condenser temperature

the plant cost is minimum when the system is run using refrigerant pair R41–R161 and maximum cost rate is involved with R170–R404A refrigerant pair. The plant cost rates for the other two refrigerant pairs are found to be in between the above two cases. The estimated annual plant cost rate of R41–R161 system varies from 83,202 to 62,429 USD within the investigated condenser temperature range of 37–55 °C. The corresponding values for R170–R161 system are 84,675 and 63,651 USD, respectively.

Effect of LTC condenser temperature on COP and exergetic efficiency

Figure 6 depicts the variations of COP and exergetic efficiency of the system with LTC condenser temperature for different refrigerant pairs. Performance assessment has been carried out keeping evaporator temperature, condenser temperature and the temperature difference in the cascade condenser temperature difference fixed at − 35 °C, 40 °C and 5 K, respectively. It is evident that the rise in LTC condenser temperature causes an increase in pressure ratio in the LTC and a decrease of the same in the HTC. As a consequence, compressors power requirement increases in the LTC and decreases in the HTC, respectively. This leads to a decrease in the COP and exergetic efficiency in LTC. However, both will increase in HTC. These two opposite trends in the two cycles increase in overall COP initially and then decrease after a certain LTC condenser temperature. Similar results were also reported by Lee et al. [7] and Roy and Mandal [23]. The exergetic efficiency is also found to follow the similar variation. The above trend is distinctly visible in the figure for systems with refrigerant pairs R41–R404A and R170–R404A. The
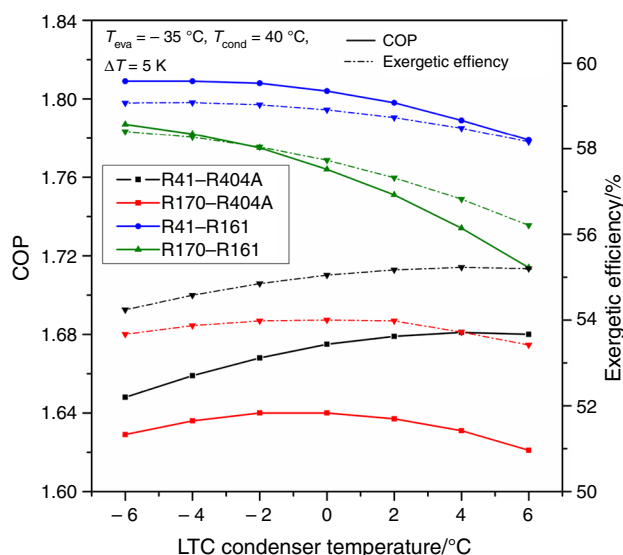
optimal LTC condenser temperatures are noted to be 0 °C and 4 °C for R41–R404A and R170–R404A combinations, respectively. The figure also indicates that the optimal points for the other two investigated refrigerant pairs can be obtained at temperatures lower than − 6 °C, which fall outside the investigated LTC condenser temperature range. It is also noticeable that higher values of COP and exergetic efficiency are achieved using the refrigerant pairs R41–R161 and R170–R161 compared to refrigerant pair R41–R404A and least values are obtained using R170–R404A pair. It can be noted that COP achieved using R41–R161 refrigerant pair is 2.7%, 7.1% and 9.8% higher than those of the systems using R170–R161, R41–R404A and R170–R404A refrigerant pairs, respectively, for a LTC condenser temperature of 2 °C. In a similar manner, the exergetic efficiency using R41–R161 is 2.5%, 6.5% and 8.8% more than the other three refrigerant pairs, respectively.

Effect of LTC condenser temperature on total plant cost

The effect of LTC condenser temperature on the total cost rate of the system is illustrated in Fig. 7. The total plant cost rate initially decreases and then again increases with the increase in LTC condenser temperature. This is due to the fact that as LTC condenser temperature increases, the compressor power in the LTC increases and at the same time, the compressor power in the HTC decreases. These two opposite trends in the LTC and the HTC will finally decide the operational cost and CO_2 penalty cost. The change in LTC condenser temperature has no significant influence on the capital and maintenance cost. The three

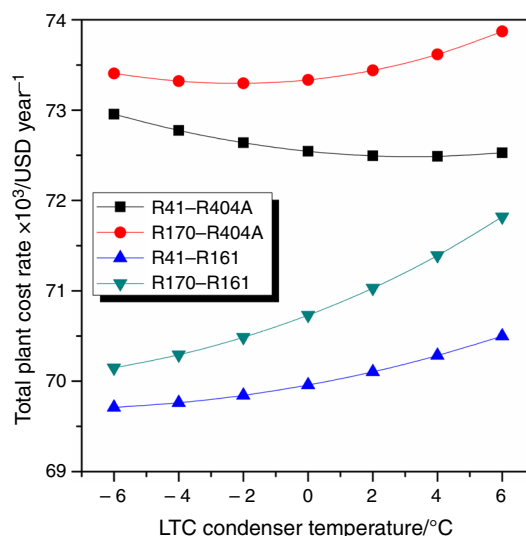**Fig. 6** Variation of COP and exergetic efficiency on LTC condenser temperature

Fig. 7 Variation of total plant cost rate on LTC condenser temperature

cost components as mentioned above finally result in initial decrease and then increase in the total plant cost rate. This variation has been observed clearly in case of R41–R404A and R170–R404A refrigerant pairs within the investigated range of LTC condenser temperature. For the other two refrigerant pairs, lowest cost rate can be observed at a LTC condenser temperature lower than − 6 °C (not shown in the figure). Similar trend was also reported by Rezayan and Behbahaninia [25] using R744–R717 refrigerant pair. It can be further observed from the figure that the minimum plant cost is associated with R41–R161 system whereas maximum cost rate is associated with the system using R170–R404A refrigerant pair. It is estimated from detailed calculation that average amounts of 2600 USD and 1800 USD per annum can be saved if refrigerant pairs R41–R161 and R170–R161, respectively, are used instead of R41–R404A.

Effect of cascade condenser temperature difference on COP and exergetic efficiency

Figure 8 shows that an increase in cascade condenser temperature difference leads to a decrease in both the COP and exergetic efficiency of the system. Simulation has been carried out keeping evaporator temperature, condenser temperature and LTC condenser temperature fixed at − 35 °C, 40 °C and 6 °C, respectively. As the cascade condenser temperature difference increases, pressure ratio and hence the compressor power in the HTC increase, but the LTC remains unaffected. Consequently, the overall COP and exergetic efficiency of the system decrease. Similar trend has also been observed by Kilicarslan and Hosez [12] using other refrigerant combinations. Among
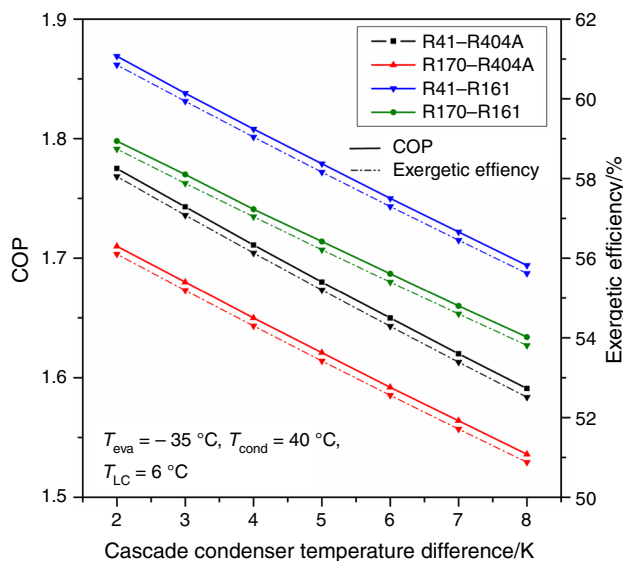
the investigated refrigerant pairs, R41–R161 provides the best thermodynamic performance. On the other hand, COP and exergetic efficiency obtained using refrigerant pair R170–R404A are not so encouraging. However, COP and exergetic efficiency obtained using refrigerant pair R41–R404A are slightly higher compared to R170–R–R404A but slightly lower compared to the other two refrigerant pairs. A 6 °C increase in cascade condenser temperature difference results in a decrease in both COP and exergetic efficiency by 10.4% and 9.5%, respectively, for the system using R41–R404A refrigerant pair. The corresponding values for R170–R404A, R41–R161 and R170–R161 refrigerant pairs are found to be 10.2% and 9.3%, 9.4% and 8.6% and 9.1% and 8.4%, respectively.

Effect of cascade condenser temperature difference on total plant cost

The effects of cascade condenser temperature difference on the total plant cost rate for the four refrigerant pairs are presented in Fig. 9. The figure shows that total plant cost rate increases almost at a constant rate with the increase in cascade condenser temperature difference for all the refrigerant pairs. This can be explained from the fact that as the cascade condenser temperature difference increases compressor power requirement increases in the HTC. As a consequence, the operational cost and the CO_2 penalty cost increase. An increase in cascade condenser temperature difference also leads to an increase in the capital and maintenance cost rate of the system. This finally results in an increase in the total plant cost rate of the system. Mosaffa et al. [27] also reported similar trend of plant cost rate variation with cascade condenser temperature difference using refrigerant pair R744–R717. Figure also shows
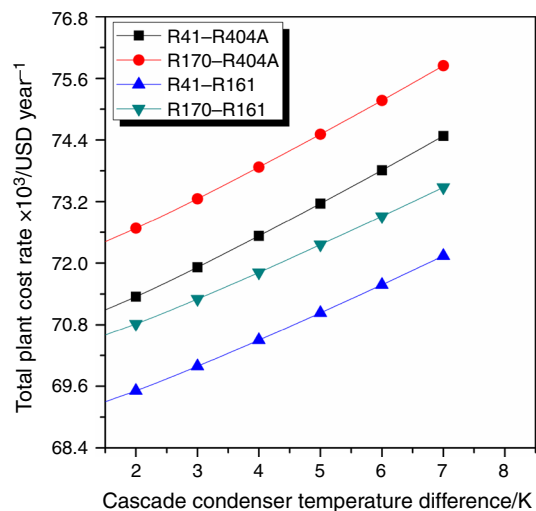

Fig. 8 Effect of cascade condenser temperature difference on COP and exergetic efficiency

Fig. 9 Effect of cascade condenser temperature difference on total plant cost rate

that use of R41–R161 refrigerant pair in the system is more economical compared to the other investigated refrigerant pairs. The plant cost using R170–R161 refrigerant pair is slightly higher than that of the R41–R161 system, whereas the CRS using R170–R404A as refrigerant pair is found to be the most expensive among the investigated systems. Predicted results also reveal that the required plant cost rates are 2.8% and 1% less when the system is simulated with R41–R161 and R170–R161 refrigerant pairs, respectively, instead of R41–R404A.

Variation of Pareto front

Figure 10a–d displays the Pareto fronts of the CRSs working with four refrigerant pairs as mentioned in the earlier sections. All the figures clearly show the conflict between the two objective functions, i.e. total plant cost rate and exergetic efficiency. The cost rate of each of the systems increases with the increase in exergetic efficiency of the system. Figure 10a shows that the annual cost rate of the R41–R404A CRS increases from 62,019 USD to 96,592 USD when the exergetic efficiency is increased from 55.1 to 59.7%. This means that 8.35% increase in exergetic efficiency leads to an increase in the cost of the system by 55.7%. Similar observations can also be made from Fig. 10b–d which shows that the cost rate increases 60.1%, 58% and 78.9% for 8.9%, 4.9% and 5.8% increase in exergetic efficiency for refrigerant pairs R170–R404A, R41–R161 and R170–R161, respectively. Though, all the points on the Pareto front are optimal points, TOPSIS decision-making method has been employed to get a unique solution for this multi-objective problem. The
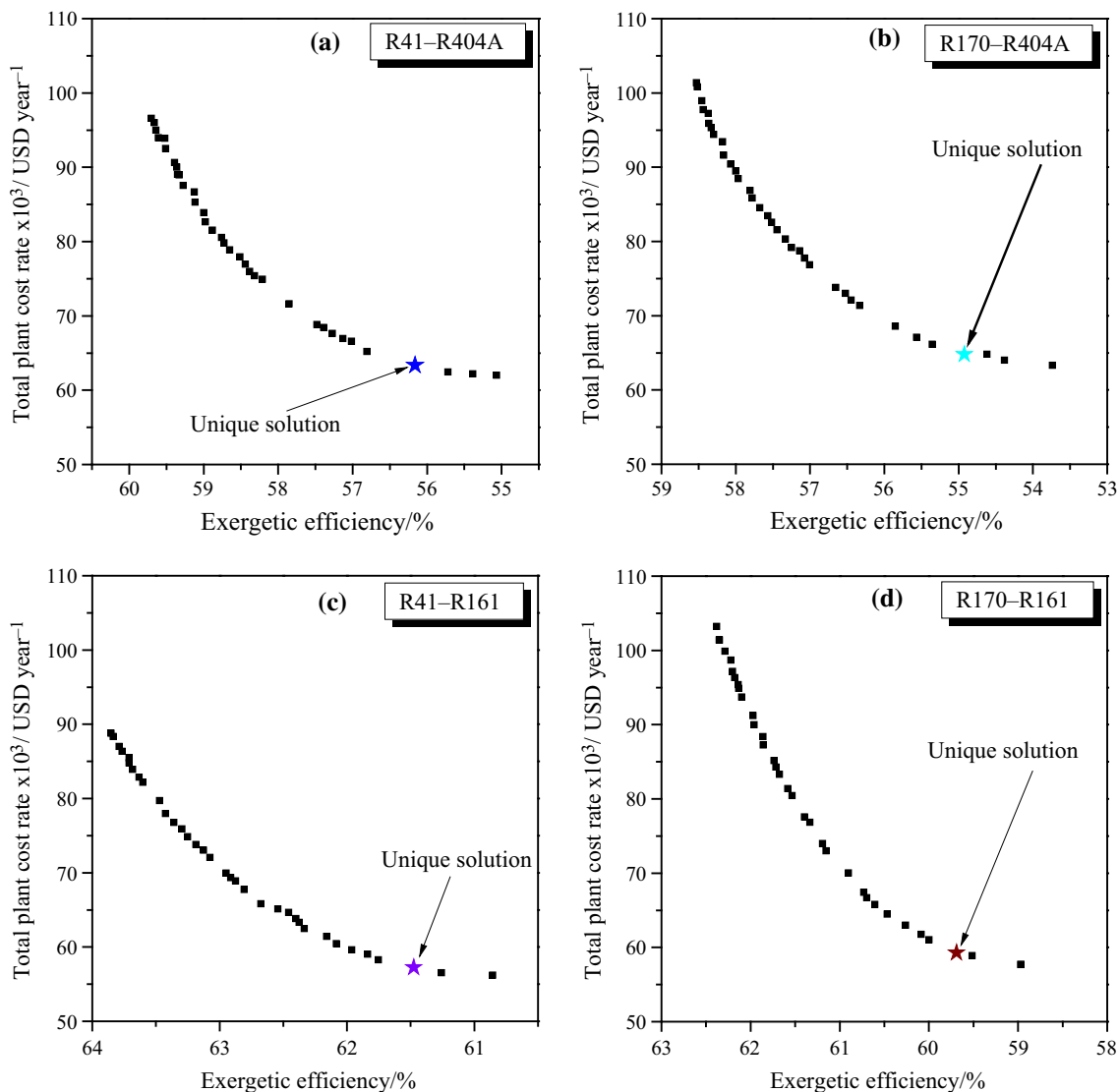

Fig. 10 Optimal Pareto front curve from multi-objective optimization of CRS with all four refrigerant pairs

Table 6 Optimum values of the operating parameters and the objectives for all four investigated refrigerant pairs obtained from the TOPSIS method

Refrigerant pair	Evaporator temperature/°C	Condenser temperature/°C	LTC condenser temperature/°C	Cascade condenser temperature difference/K	Exergetic efficiency/%	Cost rate/ USD year^{-1}
R41–R404A	− 37.6	47.2	3.8	2.1	56.2	63,346
R170–R404A	− 37.9	46.5	1	2.1	54.9	64,808
R41–R161	− 33.3	38	0.4	2.0	61.5	57,254
R170–R161	− 36.2	49.2	− 5.6	2.1	59.7	59,300

unique solution for CRS with each investigated refrigerant pair has been shown with an asterisk in the corresponding figure and is also presented in Table 6. It shows that the optimal exergetic efficiency of the system is much higher with refrigerant pair R41–R161 compared to the other refrigerant pairs particularly R41–R404A and R170–R404A pairs. It may be noted that the annual plant cost is also least at the optimal condition of exergetic efficiency in case of R41–R161 refrigerant pair. The optimal exergetic efficiency is slightly lower and the plant cost rate is slightly higher with refrigerant pair R170–R161 compared to R41–R161. But, refrigerant pair R170–R161 shows better performance compared to the remaining two refrigerant pairs (R41–R404 and R170–R404A). Exergetic efficiency of the CRSs is found to be 61.5%, 59.7%, 56.2% and 54.9% with refrigerant pairs R41–R161, R170–R161, R41–R404 and R170–R404A, respectively, at the optimal conditions. The corresponding yearly plant cost values are 57,254 USD, 59,300 USD, 63,346 USD and 64,808 USD, respectively.

Conclusions

The following conclusions can be drawn from the present simulation work on a 50-kW cooling capacity cascade refrigeration system using four different refrigerant pairs:

- COP and exergetic efficiency of the system increase with the increase in evaporator temperature. The systems with R41–R161 and R170–R161 refrigerant pairs show better thermodynamic performances than with R41–R404A pair. Improvements in COP and exergetic efficiency are found to be 4.9–7.1% and 4.5–6.6%, respectively, with R41–R161 refrigerant pair compared to R41–R404A pair for the increase of evaporator temperature from − 50 to − 21 °C. The corresponding values with R170–R161 pair are 0.1–4.1% and 0.1–3.6%, respectively.
- Plant cost rates of the systems using R41–R161 and R170–R161 pairs are less than that with system using R41–R404A pair. However, average 0.8–2.7% increase

in plant cost rate is noted with R170–R161 compared to R41–R161 refrigerant pair.
- Both COP and exergetic efficiency of the overall system decrease with the increase in condenser temperature. The annual plant cost decreases by 25% for both R41–R161 and R170–R161 systems when condenser temperature is increased by 18 K.
- An increase in LTC condenser temperature in the system leads to an initial increase and then a decrease in COP and exergetic efficiency. Refrigerant pair R41–R161 shows best performance among the tested refrigerant pairs.
- Performances of CRS deteriorate with the increase in cascade condenser temperature difference. Best performance is obtained with refrigerant pair R41–R161 followed by R170–R161 and R41–R404A pairs.
- At optimal condition, the exergetic efficiency of R41–R161 CRS is found to be 61.5% with yearly plant cost of 57,254 USD. The corresponding values for R170–R161 pair at optimal condition are 59.7% and 59,300 USD, respectively.
- R41–R161- and R170–R161-based CRSs are capable of replacing the existing R41–R404A system.
- Refrigerant R170 and R161 can be used as an alternative for refrigerant R41 and R404A in CRS due to their similar thermodynamic properties and less environmental impact.

Some previous thermodynamic performance studies have been carried out using R41–R404A as cascade refrigerant pair. However, the GWP value of R404A is much higher and it needs to be replaced by some new low GWP refrigerants. The present investigation shows that the thermo-economic performances of the system using refrigerant pairs R41–R161 and R170–R161 are superior to the refrigerant combination of R41–R404A. The investigated two refrigerant pairs are also in line with the Kigali amendment [3] which recommended the use of refrigerants having reasonably low GWP in different vapour compression refrigeration systems.

The authors are trying to simulate cascade refrigeration system using refrigerant mixture in one cycle or in both the

cycles as the next work. This may be helpful to take into account the flammability issue of R170. The experimental investigation on the similar cascade system can be carried out using different refrigerant pairs.

Compliance with ethical standards

Conflict of interest The authors declare that they have no conflict of interest.

References

1. Coulomb D, Dupont JL, Pichard A. 29th Informatory note on refrigeration technologies. The Role of Refrigeration in the Global Economy; IIR document; IIR (International Institute of Refrigeration): Paris, France. 2015.
2. Doménech RL, Alcaraz ET, López RC, Bernad JA. Experimental energetic analysis of the liquid injection effect in a two-stage refrigeration facility using a compound compressor. HVAC&R Res. 2007;13(5):819–31.
3. Heath EA. Amendment to the Montreal protocol on substances that deplete the ozone layer (Kigali amendment). Int Legal Mater. 2017;56(1):193–205.
4. Kilicarslan A. An experimental investigation of a different type vapor compression cascade refrigeration system. Appl Therm Eng. 2004;24(17–18):2611–26.
5. Di Nicola G, Giuliani G, Polonara F, Stryjek R. Blends of carbon dioxide and HFCs as working fluids for the low-temperature circuit in cascade refrigerating systems. Int J Refrig. 2005;28(2):130–40.
6. Niu B, Zhang Y. Experimental study of the refrigeration cycle performance for the R744/R290 mixtures. Int J Refrig. 2007;30(1):37–42.
7. Lee TS, Liu CH, Chen TW. Thermodynamic analysis of optimal condensing temperature of cascade-condenser in CO_2/NH_3 cascade refrigeration systems. Int J Refrig. 2006;29(7):1100–8.
8. Dopazo JA, Fernández-Seara J, Sieres J, Uhía FJ. Theoretical analysis of a CO_2–NH_3 cascade refrigeration system for cooling applications at low temperatures. Appl Therm Eng. 2009;29(8–9):1577–83.
9. Getu HM, Bansal PK. Thermodynamic analysis of an R744–R717 cascade refrigeration system. Int J Refrig. 2008;31(1):45–54.
10. Tripathy S, Jena J, Padhiary DK, Roul MK. Thermodynamic analysis of a cascade refrigeration system based on carbon dioxide and ammonia. Int J Eng Res Appl. 2014;3:6–10.
11. Messineo A. R744–R717 cascade refrigeration system: performance evaluation compared with a HFC two-stage system. Energy Procedia. 2012;14:56–65.
12. Kilicarslan A, Hosoz M. Energy and irreversibility analysis of a cascade refrigeration system for various refrigerant couples. Energy Convers Manage. 2010;51(12):2947–54.
13. Bingming W, Huagen W, Jianfeng L, Ziwen X. Experimental investigation on the performance of NH_3/CO_2 cascade refrigeration system with twin-screw compressor. Int J Refrig. 2009;32(6):1358–65.
14. Dopazo JA, Fernández-Seara J. Experimental evaluation of a cascade refrigeration system prototype with CO_2 and NH_3 for freezing process applications. Int J Refrig. 2011;34(1):257–67.
15. Belozerov G, Mednikova N, Pytchenko V, Serova E. Cascade type refrigeration systems working on CO_2/NH_3 for technological process of products freezing and storage. In IIR Ammonia Refrigeration Conference, Ohrid, Republic of Macedonia 2007 April.
16. Ma YT, Ning JH, Chen Q, Ma LR. Study on replacement and energy-saving of natural refrigerant CO_2/NH_3 cascade refrigeration cycle. In: Proceedings of the International Conference on Compressor and Refrigeration 2005.
17. Likitthammanit MA. Experimental investigations of NH_3/CO_2 cascade and transcritical CO_2 refrigeration systems in supermarkets. Stockholm: KTH School of Energy and Environmental Technology; 2007.
18. Karimabad AS. Experimental Investigations of NH_3/CO_2 cascade system for supermarket refrigeration. Master of Science Thesis, Royal Institute of Technology-Stockholm; 2006.
19. Sawalha S, Perales CC, Likitthammanit M, Rogstam J, Nilsson PO. Experimental investigation of NH_3/CO_2 CRS and comparison to R404A system for supermarket refrigeration. In 22nd IIR International Congress of Refrigeration. Beijing, China. August 2007.
20. Ouadha A, Haddad C, En-Nacer M, Imine O. Performance comparison of cascade and two-stage refrigeration cycles using natural refrigerants. In: The 22nd International Congress of Refrigeration 2007: 21–26.
21. Cabello R, Sánchez D, Llopis R, Catalán J, Nebot-Andrés L, Torrella E. Energy evaluation of R152a as drop in replacement for R134a in cascade refrigeration plants. Appl Therm Eng. 2017;110:972–84.
22. Sun Z, Liang Y, Liu S, Ji W, Zang R, Liang R, Guo Z. Comparative analysis of thermodynamic performance of a cascade refrigeration system for refrigerant couples R41/R404A and R23/R404A. Appl Energy. 2016;184:19–25.
23. Roy R, Mandal BK. Energetic and exergetic performance comparison of cascade refrigeration system using R170-R161 and R41-R404A as refrigerant pairs. Heat Mass Transf. 2019;55(3):723–31.
24. Roy R, Mandal BK. Exergy analysis of cascade refrigeration system working with refrigerant pairs R41-R404A and R41-R161. In IOP Conference Series: Materials Science and Engineering 2018;377(1):012036.
25. Rezayan O, Behbahaninia A. Thermoeconomic optimization and exergy analysis of CO_2/NH_3 cascade refrigeration systems. Energy. 2011;36(2):888–95.
26. Mosaffa AH, Farshi LG, Ferreira CI, Rosen MA. Exergoeconomic and environmental analyses of CO_2/NH_3 cascade refrigeration systems equipped with different types of flash tank intercoolers. Energy Convers Manage. 2016;117:442–53.
27. Aminyavari M, Najafi B, Shirazi A, Rinaldi F. Exergetic, economic and environmental (3E) analyses, and multi-objective optimization of a CO_2/NH_3 cascade refrigeration system. Appl Therm Eng. 2014;65(1–2):42–50.
28. Abraham JA, Mohanraj M. Thermodynamic performance of automobile air conditioners working with R430A as a drop-in substitute to R134a. J Therm Anal Calorim. 2019;136(5):2071–86.
29. Gill J, Singh J, Ohunakin OS, Adelekan DS. ANN approach for irreversibility analysis of vapor compression refrigeration system using R134a/LPG blend as replacement of R134a. J Therm Anal Calorim. 2019;135(4):2495–511.
30. Gill J, Singh J, Ohunakin OS, Adelekan DS. Exergy analysis of vapor compression refrigeration system using R450A as a replacement of R134a. J Therm Anal Calorim. 2019;136(2):857–72.
31. Gill J, Singh J, Ohunakin OS, Adelekan DS. Energy analysis of a domestic refrigerator system with ANN using LPG/TiO_2–

lubricant as replacement for R134a. J Therm Anal Calorim. 2019;135(1):475–88.

32. Paradeshi L, Srinivas M, Jayaraj S. Thermodynamic analysis of a direct expansion solar-assisted heat pump system working with R290 as a drop-in substitute for R22. J Therm Anal Calorim. 2019;136(1):63–78.

33. Paradeshi L, Mohanraj M, Srinivas M, Jayaraj S. Exergy analysis of direct-expansion solar-assisted heat pumps working with R22 and R433A. J Therm Anal Calorim. 2018;134(3):2223–37.

34. Esfe MH, Hajmohammad H, Toghraie D, Rostamian H, Mahian O, Wongwises S. Multi-objective optimization of nanofluid flow in double tube heat exchangers for applications in energy systems. Energy. 2017;137:160–71.

35. Esfe MH, Yan WM, Afrand M, Sarraf M, Toghraie D, Dahari M. Estimation of thermal conductivity of Al_2O_3/water (40%)–ethylene glycol (60%) by artificial neural network and correlation using experimental data. Int Commun Heat Mass Transf. 2016;74:125–8.

36. Esfe MH, Ahangar MR, Toghraie D, Hajmohammad MH, Rostamian H, Tourang H. Designing artificial neural network on thermal conductivity of Al_2O_3–water–EG (60–40%) nanofluid using experimental data. J Therm Anal Calorim. 2016;126(2):837–43.

37. Esfe MH, Rostamian H, Toghraie D, Yan WM. Using artificial neural network to predict thermal conductivity of ethylene glycol with alumina nanoparticle. J Therm Anal Calorim. 2016;126(2):643–8.

38. Shahsavar A, Khanmohammadi S, Toghraie D, Salihepour H. Experimental investigation and develop ANNs by introducing the suitable architectures and training algorithms supported by sensitivity analysis: measure thermal conductivity and viscosity for liquid paraffin based nanofluid containing Al_2O_3 nanoparticles. J Mol Liq. 2019;276:850–60.

39. Esfe MH, Saedodin S, Bahiraei M, Toghraie D, Mahian O, Wongwises S. Thermal conductivity modeling of MgO/EG nanofluids using experimental data and artificial neural network. J Therm Anal Calorim. 2014;118(1):287–94.

40. Afrand M, Toghraie D, Sina N. Experimental study on thermal conductivity of water-based Fe_3O_4 nanofluid: development of a new correlation and modeled by artificial neural network. Int Commun Heat Mass Transf. 2016;75:262–9.

41. Esfe MH, Ahangar MR, Rejvani M, Toghraie D, Hajmohammad MH. Designing an artificial neural network to predict dynamic viscosity of aqueous nanofluid of TiO_2 using experimental data. Int Commun Heat Mass Transf. 2016;75:192–6.

42. Ahmadi GR, Toghraie D. Energy and exergy analysis of Montazeri steam power plant in Iran. Renew Sustain Energy Rev. 2016;56:454–63.

43. Ahmadi GR, Toghraie D. Parallel feed water heating repowering of a 200 MW steam power plant. J Power Technol. 2015;95(4):288–301.

44. Ahmadi G, Toghraie D, Azimian A, Akbari OA. Evaluation of synchronous execution of full repowering and solar assisting in a 200 MW steam power plant, a case study. Appl Therm Eng. 2017;112:111–23.

45. Ahmadi G, Toghraie D, Akbari OA. Technical and environmental analysis of repowering the existing CHP system in a petrochemical plant: a case study. Energy. 2018;159:937–49.

46. Ahmadi G, Toghraie D, Akbari O. Energy, exergy and environmental (3E) analysis of the existing CHP system in a petrochemical plant. Renew Sustain Energy Rev. 2019;99:234–42.

47. Ahmadi G, Toghraie D, Akbari OA. Solar parallel feed water heating repowering of a steam power plant: a case study in Iran. Renew Sustain Energy Rev. 2017;77:474–85.

48. Calm JM, Hourahan GC. Refrigerant data update. Hpac Eng. 2007;79(1):50–64.

49. Ahamed JU, Saidur R, Masjuki HH. A review on exergy analysis of vapor compression refrigeration system. Renew Sustain Energy Rev. 2011;15(3):1593–600.

50. Bayrakçi HC, Özgür AE. Energy and exergy analysis of vapor compression refrigeration system using pure hydrocarbon refrigerants. Int J Energy Res. 2009;33(12):1070–5.

51. Navidbakhsh M, Shirazi A, Sanaye S. Four E analysis and multi-objective optimization of an ice storage system incorporating PCM as the partial cold storage for air-conditioning applications. Appl Therm Eng. 2013;58(1–2):30–41.

52. Dincer I, Rosen MA, Ahmadi P. Optimization of energy systems. New York: Wiley; 2017.

53. Mosaffa AH, Farshi LG. Exergoeconomic and environmental analyses of an air conditioning system using thermal energy storage. Appl Energy. 2016;162:515–26.

54. Wang J, Zhai ZJ, Jing Y, Zhang C. Particle swarm optimization for redundant building cooling heating and power system. Appl Energy. 2010;87(12):3668–79.

55. Klein SA, Alvarado FL. EES: Engineering equation solver for the Microsoft Windows operating system. F-Chart software; 1992.

56. Sawalha S, Suleymani A, Rogstam J. CO_2 in Supermarket Refrigeration. CO_2 Project Report Phase I, KTH Energy Technology. 2006.

57. Srinivas N, Deb K. Multiobjective optimization using nondominated sorting in genetic algorithms. Evol Comput. 1994;2(3):221–48.

58. Sanaye S, Shirazi A. Thermo-economic optimization of an ice thermal energy storage system for air-conditioning applications. Energy Build. 2013;60:100–9.

59. Sanaye S, Shirazi A. Four E analysis and multi-objective optimization of an ice thermal energy storage for air-conditioning applications. Int J Refrig. 2013;36(3):828–41.

60. Diyaley S, Shilal P, Shivakoti I, Ghadai RK, Kalita K. PSI and TOPSIS based selection of process parameters in WEDM. Periodica Polytechnica Mechanical Eng. 2017;61(4):255–60.

61. Minitab. INC. MINITAB statistical software. Minitab Release, 13.2000.

62. Xuan Y, Chen G. Experimental study on HFC-161 mixture as an alternative refrigerant to R502. Int J Refrig. 2005;28(3):436–41.

63. Han XH, Qiu Y, Li P, Xu YJ, Wang Q, Chen GM. Cycle performance studies on HFC-161 in a small-scale refrigeration system as an alternative refrigerant to HFC-410A. Energy Build. 2012;44:33–8.

64. Wu M, Yuan XR, Xu YJ, Qiao XG, Han XH, Chen GM. Cycle performance study of ethyl fluoride in the refrigeration system of HFC-134a. Appl Energy. 2014;136:1004–9.

65. Wu Y, Liang X, Tu X, Zhuang R. Study of R161 refrigerant for residential air-conditioning applications, International Refrigeration and Air Conditioning Conference. Paper 1189. 2012.